

Gamma Ray Bursts Scaling Relations to test cosmological models

S. Capozziello^{1,2}, L. Consiglio^{1,2}, M. De Laurentis^{1,2}, G. De Rosa^{1,2}, C. Perna³, D. Vivolo^{1,2}

¹*Dipartimento di Scienze Fisiche, Università di Napoli "Federico II", and ²INFN Sez. di Napoli, Compl. Univ. di Monte S. Angelo, Edificio G, Via Cinthia, I-80126, Napoli, Italy,*

³*INAF - Osservatorio Astronomico di Monte Mario, Viale del Parco Mellini 84, I-00136 Roma, Italy.*

(Dated: August 1, 2018)

Gamma ray burst (GRBs) can be used to constrain cosmological parameters from medium up to very high redshift. These powerful systems could be the further reliable distance indicators after SNeIa supernovae. We consider GRBs samples to achieve the luminosity distance to redshift relation and derive the values of the cosmographic parameters considering several possible scaling relations. GRBs, if calibrated by SNeIa, seem reliable as distance indicators and give cosmographic parameters in good agreement with the Λ CDM model. GRBs correlations with neutrino and gravitational wave signals are also investigated in view of high energy neutrino experiments and gravitational wave detectors as LIGO-VIRGO. A discussion on the GRB afterglow curve up to the visible and radio wavelengths is developed considering the possibility to use the Square Kilometer Array (SKA) telescope to achieve the first GRB-radio survey.

PACS 05.45-a, 52.35.Mw, 96.50.Fm.

Keywords: Gamma Ray Bursts; Cosmology; Gravitational Waves; Neutrinos.

I. INTRODUCTION

Observational data collected in the last fifteen years, as the anisotropy and polarization spectra of the cosmic microwave background radiation (CMBR) [1–3], the large scale structure of galaxy redshift surveys [4–7], the measurements of Baryonic Acoustic Oscillations (BAO, [8, 9]) and the Hubble diagram derived from Supernovae Type Ia (SNeIa) [10–12]), strongly support the cosmological picture of a spatially flat universe with a subcritical matter content ($\Omega_M \sim 0.3$) undergoing an accelerated phase of expansion. While the observational overview is now firmly established, the search for the motivating theory is, on the contrary, still dawning despite of several efforts and the abundance of models proposed during these years. The question is not the lack of a well established theory, but the presence of too many viable candidates, ranging from the classical cosmological constant [13, 14], to scalar fields [15, 16] and higher order gravity theories [17–22], all of them being more or less capable of fitting the available data.

As usual, adding further reliable data is the best strategy to put order in the confusing abundance of theoretical models. In particular, the extension of the observed Hubble Diagram (HD) to higher redshift z , would allow to trace the universe background evolution up to the transition regime from the accelerated dark energy era to the decelerated matter dominated phase. Moreover, being the distance modulus related to the luminosity distance and depending on the dark energy equation of state, one should go to large z in order to discriminate among different models when these predict similar curves at lower redshift. Unfortunately, SNeIa are not well suitable for this aim since their current Hubble diagram go back to $z_{max} \sim 1.4 \div 1.7$ and does not extend further than $z \simeq 2$ even for excellent space based experiments such as SNAP [23]. Unlike GRBs, due to their enormous, almost instantaneous energy release, stand out as ideal candidates to explore further redshift, the farthest one today detected at $z = 8.3$ [24]. The wide range spanned by their peak energy makes them everything but standard candles; anyway the existence of many observationally motivated correlations between redshift dependent quantities and rest frame properties [25, 28–30] offers the intriguing possibility of turning GRBs into standardizable objects as SNeIa.

Many attempts to use GRBs as cosmological distance indicators tools have been already performed (see, *e.g.*, [31–36] and refs. therein) showing the potentiality of GRBs as cosmological probes.

It is mandatory to remind that the possibility offered by GRBs to track the HD deep into the matter dominated epoch does not come for free. Two main problems are actually still to be fully addressed. First, missing a local GRBs sample, all the possible correlations have to be calibrated assuming a fiducial cosmological model to estimate the redshift dependent quantities. As a consequence, the so called *circularity problem* comes out, that is to say one wants to use GRBs scaling relations to constrain the basic cosmology, but needs the basic cosmology to get the scaling relations [37]. A well behaved distance indicator should be not only visible to high z and characterized by scaling relations with as small as possible intrinsic scatter, but its physics should be well understood from a theoretical point of view. Presently, there is no full understanding of the GRBs scaling relations so that, as a dangerous drawback, one cannot anticipate whether the calibration parameters are redshift dependent or not. Since we cannot refer to specific theoretical models, one tries to address this problem in a phenomenological way.

This review, without claim of completeness, is an attempt in this direction. We will try to summarize some scaling relations and interesting features (most of them already present in literature) that could result useful to standardize GRBs in view of cosmology. The paper is organized as follows. The main features of GRB phenomena are sketched in Sec.2. The so called *fireball model* is shortly reviewed in Sec.3. Cosmology with GRBs is widely discussed in Sec.4. Here we recall the main scaling relations that could be useful in order to figure out GRBs as possible standard cosmological indicators. In particular, we discuss the correlation analysis in view of testing cosmological models. Implication for particle astrophysics (i.e. high energy neutrinos) and gravitational radiation are taken into account in Sec.5. Sec.6 is devoted to the GRB radio emission which could be extremely important to accomplish the luminosity curve of these objects in the whole electromagnetic spectrum. Conclusions are drawn in Sec.7.

II. THE GAMMA-RAY BURST PHENOMENON

GRBs are extremely powerful flashes of γ -rays which occur approximately once per day and are isotropically distributed over the sky [38]. The variability of the bursts on time scales as short as a millisecond and indicates that the sources are very compact, while the identification of host galaxies and the measurement of redshifts for more than 100 bursts have shown that GRBs are of extra-galactic origin. GRBs are grouped into two broad classes by their characteristic duration and spectral hardness: *long* and *short* GRBs [41, 42]. Moreover, cosmological GRBs are very likely powerful sources of high energy neutrinos and gravitational waves. According to the current interpretation of GRB phenomenology, the γ -ray emission is due to the dissipation of the kinetic energy of a relativistically expanding fireball [38]. The physical conditions allow protons to be accelerated to energies greater than 10^{20} eV according to the Fermi mechanism [43–46]. Such protons cannot avoid interactions with fireball photons, starting a photo-meson production process that generate very high energy neutrinos and γ -rays [47].

The occurrence of gravitational wave bursts (GWBs) associated with GRBs is a natural consequence of current models for the central engine [48]. For instance, GRBs can be produced by classes of supernovae, known as *collapsars* or *hypernovae*, when a massive star collapses to form a spinning black hole; in the meantime the remaining core materials form an accreting torus with high angular momentum [49, 50]. Another interesting scenario is a neutron star and black hole coalescing system ($\sim 7M_{\odot}$) where the disruption of the neutron star, caused by the rapidly rotating black hole, will also form a torus emitting a large amount of energy ($\sim 0.1M_{\odot}c^2$) both in gravitational and electromagnetic waves [49].

According to the fireball model, GRB afterglows are the result of a shock pushed into the ambient medium by an extremely relativistic outflow from the GRB. A conducting fireball expanding at relativistic speed into an ambient magnetic field generates a rapidly changing electric current which emits coherent electromagnetic radiation at radio frequencies. The critical frequency (upper limit of the emission) strongly depends on the Lorentz factor of the expansion. Wide radio observations of GRB afterglows would provide essential and unique information to constrain the physical models by completing the coverage of the spectral energy distribution and following the behavior up to much later times than any other wavelength.

Due to the above processes, GRBs are the most powerful phenomena of the universe located at cosmological distances [38, 51]. They were discovered in the late 60's by the military VELA satellites, as *X-ray* bursts and γ -ray photons occurring at random place and date in the sky [52]. Further observations led to the discovery of slowly fading *X-ray*, optical and radio afterglows following the burst of photons of the *prompt* phase, and the identification of host galaxies at cosmological distances.

Specifically, the prompt emission phase of long bursts lasts typically 20 seconds, and more than two seconds. The short bursts have a shorter duration, typically of 0.2 seconds [53, 54]. Both classes present an afterglow emission, rather similar [55]. The difference between the prompt phases of short and long GRBs derives from the nature of the progenitor. The progenitors of most short GRBs are widely thought to be mergers of neutron star binaries (NS-NS) or neutron star-black hole (NS-BH) binaries [56]. A small fraction (up to $\simeq 15\%$) of short GRBs are also thought to be due to giant flares from a local distribution of soft-gamma repeaters [57–59]. Long GRBs, on the other hand, are associated with core-collapse Supernovae [60–63]. As said above, both the merger and supernova scenarios result in the formation of a stellar-mass black hole with accretion disk. The emission of gravitational radiation and neutrinos are expected in this process [64, 65]. GRBs are also classified on the basis of other electromagnetic properties. One can, for example, consider the optical brightness of the afterglow, distinguishing *dark* bursts, having no optical afterglow emission [66, 67]; or *X-ray Flashes* (which have no emission in the γ -rays, the prompt being reduced to a burst of soft *X-ray* photons) [68]. These classifications are based on observations and can be related to the properties of the medium in which the burst develops or to the geometry of the explosion [66, 69, 70].

III. THE FIREBALL MODEL

The *fireball model* is based on an "central engine" highly energetic which produces a relativistic particle outflow. Since the opacity is very high, this "engine" is well hidden from direct observations and it is very difficult to determine what is the source of this mechanism from present observations. Also the afterglow discovery does not add further information in this direction, leading only to some circumstantial evidences on the nature of the sources. The energy from the central source is transported relativistically to distances larger than 10^{16} cm where the system is optically thin. The fireball particles flux is not emitted at a constant rate by the central engine but two jets back to back occur in the near of the central engine. Such jets are made up of photons, baryons and e^-/e^+ pairs that accelerate the surrounding material by forming concentric and consecutive shells. During the acceleration process, some shells are emitted with a higher velocity respect to others. Faster shells interact with slower ones causing an inelastic shock which accelerates electrons producing a gamma emission at high energy. This mechanism called *internal shock* powers the GRB itself producing the prompt emission [71]. Subsequently, the fireball, during its expansion, bumps into external medium which can be the interstellar medium or the dense stellar wind produced by the progenitor of GRB. External shocks arise due to the interaction of the relativistic matter with the surrounding matter, and cause the GRB afterglow. These shocks or blast waves are the relativistic analogues of supernova remnants. The shock will produce a magnetic field within the top of the jet, so that the electrons will start to emit synchrotron radiation. When the external forward shock is formed, a reverse shock is produced moving back into the ejecta. This reverse shock can produce a bright optical flash about one minute after the burst, and a radio flare about one day after the burst. The brightness of the reverse shock emission decays very rapidly, after which the forward shock dominates. The relativistic outflow is not spherical but collimated. Since the shock decelerates while it is sweeping up mass, a few days after the burst, the synchrotron emission angle of the electrons becomes equal to the collimation angle of the outflow, the so-called jet-break time. After this moment the collimated outflow spreads and becomes spherical after a few months after the burst. At the same time that the outflow becomes spherical, the blast wave becomes sub-relativistic and will eventually enter the classical regime. GRBs occur at a rate of about one per 10^6 years per galaxy [72] and the total energy is $\sim 10^{52}$ ergs. These estimates are obtained assuming isotropic emission. The jet beaming angle θ_{jet} can changes the rate estimation by a factor $\frac{4\pi}{\theta_{jet}^2}$ in the rate, and by a factor of $\frac{\theta_{jet}^2}{4\pi}$ in the fireball total energy. The luminosity per unit solid angle along the jet axis is different from the one emitted on axis. A strongly off-axis position of a detector would not allow the prompt GRBs observation so that it would be possible to see (in case of a long GRB) only the late afterglow [73]. A further constraint on fireball model is the inner engine capability of accelerating $\sim 10^{-5}M_{\odot}$ to relativistic energies.

One can imagine various scenarios in which 10^{52} ergs are generated within a short time. The condition that such energy should be converted into a relativistic flow is quite difficult since it needs a system with a very low baryonic load. This requirement prefers models based on electromagnetic energy transfer or electromagnetic energy generation as these could more naturally satisfy this condition (see [74]).

IV. COSMOLOGY BY GRBS

The cosmological origin of GRBs has been confirmed by several spectroscopic measurements of their redshifts, distributed in the range $z \in 0.1 \div 8.3$. This property makes GRBs suitable for investigating the far universe. Indeed, they can be used to constrain the geometry of the present day universe and the nature and evolution of dark energy by testing the cosmological models in a redshift range hardly achievable by other cosmological probes. Moreover, the use of GRBs as cosmological tools could probe the ionization history of the universe, the intergalactic medium properties and the formation of massive stars in the early universe. The fact that GRBs are detected up to very high redshifts makes it possible an attempt to use them as standard candles in a similar way as SNeIa, because they have a very wide range of isotropic equivalent luminosities and energy outputs. Several suggestions have been made to calibrate them as better standard candles by using correlations between various properties of the prompt emission, and in some cases also the afterglow emission. While there is good motivation for such cosmological applications of GRBs, there are many practical difficulties.

Indeed, a serious problem that arises is the intrinsic scarcity of the nearby events which introduces a bias towards low/high values of GRB observables. As a consequence, it is not immediate to extrapolate the correlations to low- z events. A further problem is related to the fact that, due to the unknown flux limit, the GRB ensemble suffer from the well known degradation of sampling as a function of redshift. One might also expect a significant evolution of the intrinsic properties of GRBs with redshift (also between intermediate and high redshifts) which can be hard to decouple from cosmological effects. Finally, in order to calibrate the observed correlations, it is mandatory to assume

a cosmological model (luminosity distance vs redshift) in order to convert the observed bolometric peak flux P_{bolo} or bolometric fluence to isotropic absolute luminosity L or to a total collimation corrected energy E_γ . The use of a cosmological model to perform the calibration, in turn, creates a circularity problem and a model dependence of the obtained calibration.

Despite of these difficulties, the potential advantages to obtain approximate standard candles at high redshifts have generated an intense activity in the direction to test GRBs as cosmological indicators [30, 31] as well as to constrain cosmological parameters by them [25, 75–77]. This means that GRB cannot be alternative to the SNeIa or to other cosmological probes, but they can be complementary to them due to their wide redshift distribution and evolution properties. The goal is to use them to remove the degeneracies in the values of cosmological parameters, today obtained only at medium and low redshift (see for example [26, 27]).

A. The standard candles test

The standard methods to test cosmological models, are:

- the luminosity distance test (mainly applied to SNeIa);
- the angular size distance test (used also for Cosmic Microwave Background (CMB) anisotropies);
- the volume test based on galaxy number count.

In general, given an object with a certain luminosity L , not evolving with cosmic time, and measured flux F , one can define its luminosity distance $D_L = \sqrt{\frac{L}{4\pi F(z)}}$ which is related to the radial coordinate r of the Friedman-Robertson-

Walker metric by $D_L = \frac{r}{a(\tau)} = r(1+z)$, where $a(\tau)$ is the scale factor as a function of the comoving time, $\tau = tH_0$.

D_L depends on the expansion history and curvature of the universe through the radial coordinate r . By measuring the flux of 'standard candles' as a function of redshift, $F(z)$, the luminosity distance test is achieved by comparing D_L , obtained from the flux measurement, with $D_L(\bar{p})$ predicted by the cosmological model, where \bar{p} is a set of cosmological parameters (*e.g.*, the matter density parameter Ω_M , the cosmological density parameter Ω_Λ and the normalized Hubble constant h [78, 79]). This test has been largely used with SNeIa [79]. The high peak luminosity (*i.e.* $\sim 10^{10} M_\odot$) of SNeIa makes them detectable above $z > 1$.

Several intrinsic correlations between temporal or spectral properties and GRB isotropic energetics and luminosities have been considered as a possibility to use GRBs as cosmological indicators [80]. The constraints on the cosmological parameters obtained by the luminosity distance test applied to GRBs are less severe than those obtained by SNeIa. This is mainly due to the presently still limited number of GRBs with well determined prompt and afterglow properties that can be used as standard indicators.

B. GRB luminosities and energetics

The luminosity L and the energy E of GRBs with well know redshifts can be evaluated by the peak flux P and the flux integrated over the burst duration (*i.e.* the fluence S). If GRBs emit isotropically, the energy radiated during their prompt phase is $E_{iso} = \frac{4\pi D_L^2 S}{(1+z)}$ where the term $(1+z)$ accounts for the cosmological time dilation effect while the isotropic luminosity is $L_{iso} = 4\pi D_L^2 P$. The bolometric luminosity is often computed by combining the peak flux (relative to the peak of the GRB light curve) with the spectral data derived from the analysis of time integrated spectrum. As discussed in [72], this is strictly correct only if the GRB spectrum does not evolve in time during the burst [81]. A considerable reduction of dispersion of GRBs energetics has been found in [82] (later confirmed in [83]) when they are corrected for the collimated geometry of these sources. Theoretical considerations on the extreme GRB energetics under the hypothesis of isotropic emission [84, 85] led to the hypothesis that, similarly to other sources, also GRBs might be characterized by a jet. In the classical scenario, the presence of a jet [86–88] affects the afterglow light curve which should present an achromatic break a few days after the burst. The observation of the afterglow light curves allows to estimate the jet opening angle θ_{jet} from which the collimation factor can be computed, *i.e.* $f = (1 - \cos \theta_{jet})$. This geometric correction factor, applied to the isotropic energies [82], led to a considerable reduction of the GRB energetics and of their dispersion.

C. The intrinsic correlation of GRBs

Several empirical relations between observable properties of the prompt emission have been discovered during the recent years. The luminosity relations are connections between measurable parameters of the light curves and/or spectra with the GRB luminosity. The calibration consists in a fit of the luminosity indicator versus the luminosity in logarithmic scale. This calibration process needs to know burst's luminosity distance in order to convert P_{bolo} to L and this can be done only for bursts with measured redshifts. The crucial point is that conversion from observed redshift to luminosity distance requires some adopted cosmological parameters to be calibrated separately.

If we are interested in calibration for purposes of GRB physics, then it will be fine to adopt the calibration from some fiducial cosmology. But if we are interested in testing the cosmology, then we have to use the calibration for each individual cosmology being tested. For a particular cosmology, the theoretical shape of HD has to be compared with the observed shape when the burst distances are calculated based on calibrations for that particular cosmology. Thus, any test of cosmological models with a GRB-HD will be a simultaneous fit of the parameters in the calibration curves and the cosmology. In the following subsections these correlations are summarized.

1. The lag-luminosity correlation $\tau - L_{\text{iso}}$

Results from BATSE satellite [89] on the analysis of the light curves of GRBs led to the discovery of spectral lags, *i.e.* the difference in arrival time of high and low energy photons. It is assumed positive when high energy photons arrive earlier than the low energy ones. Usually the spectral lag is extracted between two energy bands in the observed reference frame. Since GRBs are redshift dependent, the two energy bands extracted can refer to a different couple of energy bands in the GRBs absolute frame; in this way energy depends on the spectral lag considered. Time lags typically range between 0.01 and 0.5s (even few second lags have been observed [90]) and there is no evidence of any trend, within multi peaked GRBs, between the lags of the initial and the latest peaks [91]. It has been proposed that lags are a consequence of the spectral evolution [92], typically observed in GRBs [93], and they have been interpreted as due to radiative cooling effects [94]. Other interpretations concern geometric and hydrodynamic effects [95, 96] within the standard GRB model. In particular, the analysis of GRB temporal properties with known redshifts revealed a tight correlation between their spectral lags (τ) and the luminosity (L_{iso}) [97]. Furthermore, the $\tau - L_{\text{iso}}$ correlation has been used as a pseudo-redshift indicator to estimate z for a large population of GRBs [98] and also to study the GRB population properties, like as jet opening angle, luminosity function and redshift distribution within a unifying picture [90].

2. The variability-luminosity correlation $V - L_{\text{iso}}$

GRB temporal structure shows several shapes: they exhibit a variation from a single smooth pulse to very high complex light curves with a lot of fancy pulses with different amplitudes time duration. Also the afterglow emission shows some variability on timescales [99, 100]. The analysis of large samples of bursts also showed the existence of a correlation between the GRB observer frame intensity and its variability [101]. Several scenarios have been proposed to provide an explanation of GRBs temporal variability. The most accredited mechanism asserts that light curves variability would be due to the irregularity of the central engine. Alternatively, an external origin of the observed variability as due to the shock formation by the interaction of the relativistically expanding fireball and variable size interstellar medium clouds is proposed in [102]. Fenimore and Ramirez-Ruiz [103] and Reichart et al., [104] found a correlation between GRB luminosities L_{iso} and their variability V : more luminous bursts have a more variable light curve. The $V - L_{\text{iso}}$ correlation has been recently updated [105] with a sample of 31 GRBs with measured redshifts. This correlation has also been tested [106] with a large sample of 155 GRBs with only a pseudo-redshift estimate (from the lag-luminosity correlation [37, 98]). An even tighter correlation (*i.e.* with a reduction of a factor 3 of its scatter) has been derived [107] by slightly modifying the definition of the variability first proposed in [104]. Recently Zhang and Yan [108] proposed Internal- Collision-Induced-Magnetic Reconnection and Turbulence model of GRBs prompt emission in the Poynting-flux-dominated regime. This model is based on a central engine with powered, magnetically dominated outflow which self interacts and triggers fast magnetic turbulent reconnection that powers the observed GRBs. This model has two variability components: one slow component is related to the central engine activity which is responsible of the visually apparent broad pulses in GRBs light curves; the other fast one is associated with relativistic magnetic turbulence responsible of the faster variabilities overlapping the broad pulses. It is fundamental to use rigorous approaches to study GRBs light curves in order to investigate superpositions of multiple variability components. Power density spectrum is, however, the most used tool to study the temporal behavior of varying astronomical objects [109].

3. The spectral peak energy-isotropic energy correlation $E_{peak} - E_{iso}$

The $E_{peak} - E_{iso}$ relation is one of the most latest intriguing discovery related to GRBs and could have several implications on the understanding of the emission mechanism of the burst and on the possibility to use GRBs for cosmology. Even before large samples of burst with measured redshift were available, it was suggested that the $E_{peak} - E_{iso}$ were correlated [110]. Hereafter the measurements of some redshift Amati et al. [111] reported the correlation between the isotropic equivalent bolometric energy output in γ -rays, E_{iso} , and the intrinsic peak energy of the νF_ν spectrum, E_{peak} . This result was based on a sample of 12 BeppoSAX bursts [112] with known redshifts. Ten additional bursts detected by HETE II ([113–115]) supported this result and extended it down to $E_{iso} \sim 10^{49}$ ergs (see also [79]). The $E_{peak} - E_{iso}$ correlation has been updated with a sample of 43 GRBs (comprising also 2XRF) by estimating z and the spectral properties [116]. The theoretical interpretations of $E_{peak} - E_{iso}$ correlation attribute it to geometrical effects due to the jet viewing angle with respect to a ring-shaped emission region [117, 118] or with respect to a multiple sub-jet model structure which also takes into account for the extension of the above correlation to the X-ray rich (XRR) and XRF classes [119, 120]. A different explanation for the $E_{peak} - E_{iso}$ correlation concerns the dissipative mechanism responsible for the prompt emission [121]: if the peak spectral energy is interpreted as the fireball photospheric thermal emission comptonized by some mechanism (*e.g.* magnetic reconnection or internal shock) taking place below the transparency radius, the observed correlation can be reproduced.

4. The peak spectral energy-isotropic luminosity correlation $E_{peak} - L_{iso}$

The E_{peak} and L_{iso} has been discovered [122] with a sample of 16 GRBs. A wider sample of 25 GRBs confirmed this correlation [72]. As already said, the luminosity L_{iso} is defined by combining the time-integrated spectrum of the burst with its peak flux (also E_{peak} is derived using the time-integrated spectrum). It has been demonstrated that GRBs are characterized by a considerable spectral evolution [92]. If the peak luminosity is obtained only considering the spectrum integrated over a small time interval ($\sim 1s$) centered around the peak of the burst light curve, we find a larger dispersion of the $E_{peak} - L_{iso}$ correlation (see [123]). This suggests that, the time averaged quantities (*i.e.* the peak energy of the time-integrated spectrum and the "peak-averaged" luminosity) are better correlated than the "time-resolved" quantities. Combining the lag-luminosity and the variability- luminosity relations of nine GRBs to build their Hubble diagram it is possible to consider GRBs as powerful cosmological tools [37, 75].

5. The peak energy-collimation corrected energy correlation $E_{peak} - E_\gamma$

By using a large sample of burst with spectroscopical measured redshift, assuming a homogeneous circumburst medium, Ghirlanda et al. [113] estimated the jet opening angle θ_{jet} and the related E_γ defined as $E_{iso}(1 - \cos\theta_{jet})$. They discovered a very tight correlation between E_γ respect E_{peak} . Such correlation links the GRB prompt emission energy, corrected for the burst geometry, to its peak frequency. By adding a large sample of GRB, some of which also discovered by SWIFT [127] and, at least, by another InterPlanetary Network (IPN) satellite [128] in order to estimate the peak energy, this correlation has been confirmed. Recently, Nava et al., in [124], reconsidered and updated the original sample of GRBs with firm estimate of their redshift, spectral properties and jet break times. One possible explanation to see these events out of their jet opening angle in such way that they appear off-beam-axis in both E_{peak} and E_{iso} has been proposed (see also [125, 126]). Otherwise, alternative possibility [129, 130] have been put forward. Nava et al. [124] have calculated $E_{peak} - E_\gamma$ correlation by assuming an external medium distributed with an r^{-2} density profile, finding an even tighter correlation with respect to that one obtained assuming an homogenous circumburst density. The linearity of the Ghirlanda E_{peak} correlation implies that it is invariant under transformation from the source rest frame to the fireball comoving frame. A consequence of this property is that the number of total photons emitted in different GRBs is constant and correspond to $N_\gamma \sim 10^{57}$. This number is very close to the number of baryons in one solar mass. This property could have an important implication in the dynamics and radiative processes of GRBs.

6. The isotropic luminosity-peak energy-high signal timescale correlation $L_{iso} - E_{peak} - T_{0.45}$

A correlation involving three observables of the GRB prompt emission is discussed in [31]: the isotropic luminosity L_{iso} , the rest frame peak energy E_{peak} and the rest frame "high signal" timescale $T_{0.45}$. This latter parameter has been previously used to characterize the GRB variability (*e.g.* [104]) and represents the time crosses by the brightest 45% of the total counts above the background. Through the analysis of 19 GRBs, for which L_{iso} , E_{peak} and $T_{0.45}$

could be derived, in [31] it is found that $L_{iso} \propto E_{peak}^{1.62} \cdot T_{0.45}^{-0.49}$ with a very small scatter. The $L_{iso} - E_{peak} - T_{0.45}$ correlation is based on prompt emission properties only and it is sufficiently tight to standardize GRB energetics having some interesting consequences:

1. it represents a powerful (redshift) indicator for GRBs without measured redshifts, which can be computed only from the prompt emission data (spectrum and light curve);
2. it can be considered a cosmological tool which is model independent (differently from the $E_\gamma - E_{peak}$ correlation which relies on the standard GRB jet model [31]);
3. it is "Lorentz invariant" for standard fireballs, *i.e.* when the jet opening angle is $\theta_{jet} > \frac{1}{\Gamma}$.

These features could be extremely interesting in view of using GRBs as cosmological distance indicators.

7. The peak energy-isotropic energy-jet break time correlation $E_{peak} - E_{iso} - t_{break}$

All the above correlations have been derived assuming that GRBs emit isotropically. However, the hypothesis that GRB fireballs are collimated was proposed for GRB 970508 [84] and subsequently for GRB 990123 as a possible explanation of their very large isotropic energy [85]. The collimated GRB model predicts the appearance of an achromatic break in the afterglow light curve which, after this break time, decreases with respect to the time [86, 87]. Since the fireball photon emission depends on the relativistic beaming angle, the observer receives the photons within a cone with aperture $\theta_\Gamma \propto \frac{1}{\Gamma}$, where Γ is the bulk Lorentz factor of the material responsible for the emission. During the afterglow phase, the fireball is decelerated by the circumburst medium and its bulk Lorentz factor decreases, *i.e.* the beaming angle θ_Γ increases with time. As the beaming angle equals the jet opening angle, $\theta_\Gamma \sim \frac{1}{\Gamma} \sim \theta_{jet}$, a critical time is reached. With this assumptions, the jet opening angle θ_{jet} can be estimated through this characteristic time [87], *i.e.* the so called jet-break time t_{break} related to the afterglow light curve. Typical t_{break} values ranges from 0.5 to 6 days [82, 83, 113]. The jet opening angle can be derived from t_{break} in two different scenarios (*e.g.* [131]). Another empirical correlation links the jet break time t_{break} with E_{iso} and peak energy E_{peak} .

As discussed in [124], the model dependent $E_{peak} - E_\gamma$ correlations (*i.e.* derived under the assumption of a standard uniform jet model and either for a uniform or a wind circumburst medium) are consistent with this completely empirical correlation. This result, therefore, reinforces the validity of the scenario within which they have been derived, *i.e.* a relativistic fireball with a uniform jet geometry which is decelerated by the external medium, with either a constant or an r^{-2} profile density. Similarly to what has been done with the isotropic quantities, we can explore if the collimation corrected $E_{peak} - E_\gamma$ correlation still holds when the luminosity, instead of the energy, is considered.

D. Cosmological analysis of GRB correlations

A preliminary step in the analysis of correlations mentioned above is the determination of the luminosity L or the collimated energy E_γ entering as y variable in the $y-x$ scaling laws $\log y = a \log x + b$. This is a linear relation which can be fitted in order to determine the calibration parameter a and b . Since, there is still no theoretical model explaining any correlations in term of GRB physics, one would expect that the wide range of GRB properties makes the objects scatter around this (unknown) idealized model. Consequently, the above linear relations will be affected by an intrinsic scatter σ_{int} which has to be determined together with the calibration coefficients (a, b). As a first step, it is necessary to determine the GRBs luminosity distance over a redshift range where the linear Hubble law does not hold anymore. In such a way the luminosity distance can be estimated as:

$$d_L(z) = \frac{c(1+z)}{H_0} \int_0^z \frac{dz'}{E(z')} \quad (1)$$

where $H_0 = 100h$ km/s/Mpc is the present day Hubble constant and $E(z) = H(z)/H_0$ is the dimensionless Hubble parameter which depends on the adopted cosmological model thus leading to the well known *circularity problem*.

Several strategies have been considered to take in to account this problem [37]. The most easy one is to assume a fiducial cosmological model and determine its parameters by fitting, *e.g.*, the SNeIa Hubble diagram. One adopts the Λ CDM model as fiducial one thus setting:

$$E^2(z) = \Omega_M(1+z)^3 + \Omega_\Lambda \quad (2)$$

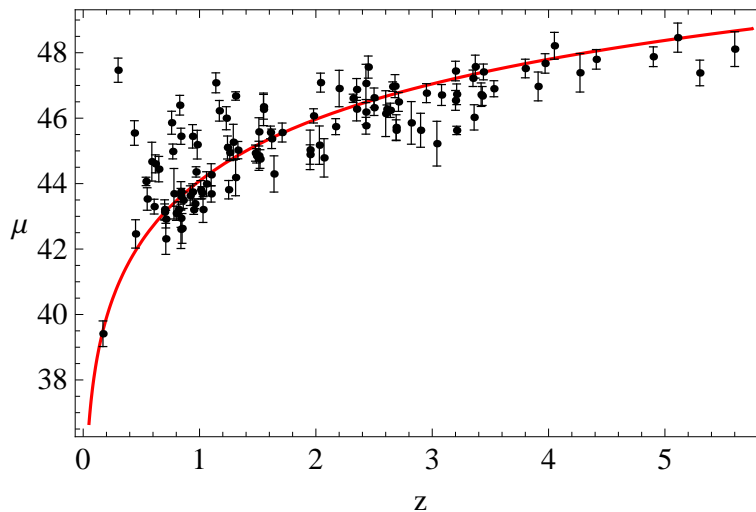


Figure 1: GRB Hubble diagram averaged over different 2D correlations derived by using calibration on the fiducial Λ CDM model [37].

where $\Omega_\Lambda = 1 - \Omega_M$ because of the spatial flatness assumption.

It is nevertheless worth stressing that a different cosmological model would give different values for $d_L(z)$ and hence different values for (L, E_γ) thus affecting the estimate of the calibration parameters (a, σ_{int}) . A first attempt to a model independent approach is to resort to cosmography [35, 132, 133], *i.e.*, to expand the scale factor $a(t)$ to the fifth order and then consider the luminosity distance as a function of the cosmographic parameters. Indeed, such a kinematic approach only relies on the validity of assumption of the Robertson-Walker metric, while no assumption on either the cosmological model or the theory of gravity is needed since the Friedmann equations are never used. A further step to a completely model independent approach is the estimation of the GRBs luminosity distances by using the SNeIa as distance indicator based on the naive observations that a GRB at redshift z must have the same distance modulus of SNeIa having the same redshift [37]. As instance one could interpolate the SNeIa HD providing the value of distance modulus for a subsample of GRBs with redshift $z \leq 1.4$ which can then be used to calibrate the correlations parameters [32, 37, 134, 135]. Assuming that this calibration is redshift independent, one can then build up the HD at higher redshifts using the calibrated correlations for the remaining GRBs in the sample.

Once the calibration parameters for a certain $y-x$ correlation have been obtained, it is then possible to estimate the distance modulus of a given GRB from the measured value of x . Indeed, for a given y , the luminosity distance is:

$$d_L^2(z) = \frac{y}{\kappa}, \quad (3)$$

where $\kappa = 4\pi P_{bol}$, $\kappa = 4\pi S_{bol} F_{beam}/(1+z)$ (F_{beam} is the beaming factor $(1 - \cos\theta_{jet})$ and $\kappa = 4\pi S_{bol}/(1+z)$ for $y = L$, $y = E_\gamma$ and E_{iso} , respectively. Using the definition of distance modulus $\mu(z) = 25 + 5 \log d_L(z)$ and estimating y from x through the $y-x$ correlation, we then get:

$$\mu(z) = 25 + \frac{5}{2} \log \left(\frac{y}{\kappa} \right) = 25 + \frac{5}{2} (a \log x + b - \log \kappa) \quad (4)$$

where (a, b) are the best fit coefficients for the given $y-x$ correlation. Eq.(4) allows to compute the central value of the distance modulus relying on the measured values of the GRB observables, *i.e.*, the ones entering the quantity κ , and the best fit coefficients (a, b) of the used correlation. Moreover, each correlation is affected by an intrinsic scatter which has to be taken into account in the total error budget.

In Fig. 1, it is reported the GRB Hubble diagram obtained by using different correlations and different calibration methods (for details see [37]). The red solid line is the expected $\mu(z)$ curve for the fiducial Λ CDM model.

From the picture, it is evident that the HD derived from GRBs reasonably follow the Λ CDM curve although with a non negligible scatter. The scatter becomes significantly larger in the range $0.4 \leq z \leq 1.4$ since the distance modulus $\mu(z)$ for a set of GRBs lies above the Λ CDM prediction. One could conjecture a failure of the theoretical model, but there is a set of points which are difficult to adapt with any reasonable dark energy model.

V. IMPLICATIONS FOR PARTICLE ASTROPHYSICS

As said above, a part electromagnetic emission, GRBs are sources of high-energy beams of particles and possible gravitational wave emitters. Below we will sketch these important implications for astroparticle physics and the possibility to complete the GRB light curve by studying radio emissions.

A. High energy neutrinos

According to the fireball model, shock accelerated protons interact with low energy radiation (photons in the range of KeV-MeV), leading to the production of ultrahigh energy pions, kaons and neutrons through the processes $p\gamma \rightarrow \pi^{\pm,0}X$ and $p\gamma \rightarrow K^{\pm,0}X$, where X can be a neutron. The ultrahigh energy mesons and neutrons, in turn, decay into high energy neutrinos/antineutrinos or photons and other secondary products. Because of the high magnetic field inside GRBs, charged pions, kaons and muons loose energy significantly before decaying into neutrinos. On the other side, the relativistic neutrons remain unaffected and decay into high energy antineutrinos, protons and electrons.

Three phases of non-thermal emission are expected: precursor phase preceding the burst [136], the prompt emission [45, 47] and afterglow emission [137]. Fig. 2 shows a schematic view of the modeled neutrino emissions from GRBs during the three phases (bottom row). Also the corresponding electromagnetic outputs are shown (top row).

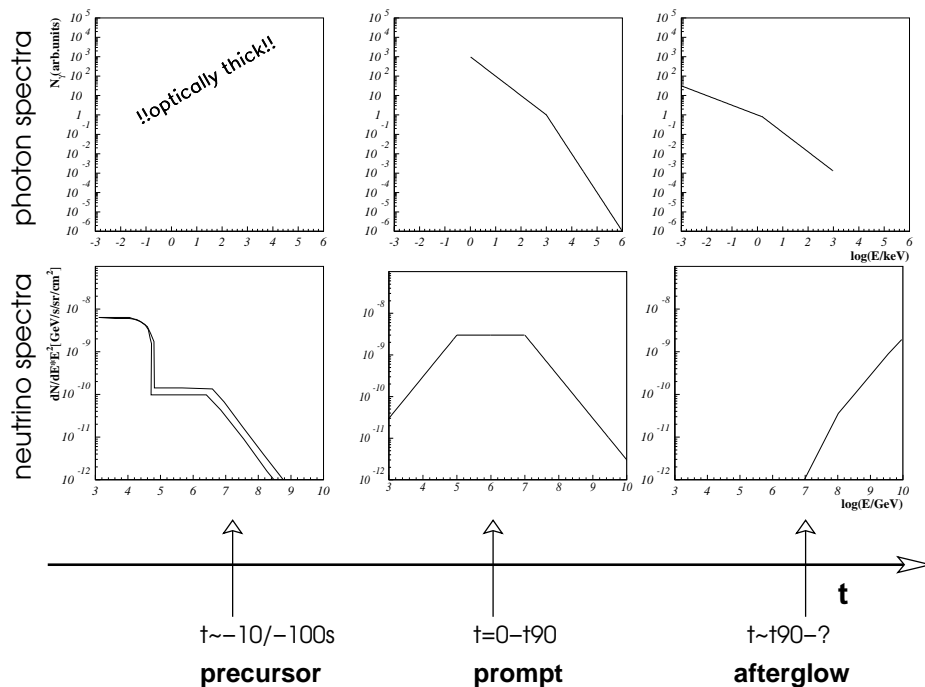


Figure 2: Overview of different neutrino production scenarios during the three different phases of a GRB emission. The corresponding electromagnetic output is indicated schematically as well. The different flux models are described in the text [138].

- A *precursor SNR (supernova remnant) model* of GRBs has been developed in [136]. The basic idea is that a shock is formed during the collision between the pre-GRB matter and the wind of the central pulsar or the SNR shell. In this state, the burst is opaque to photon emission and shock surroundings represent a good target for neutrino production by shock-accelerated protons interacting with thermal X-rays in the sub-stellar jet cavity. The shocks happen at smaller radii with respect to the prompt emission and at lower Lorentz boost factors Γ . The neutrino signal could also be accompanied by a signal in the far infrared. The low energy part of the neutrino spectrum is due to neutrino production in pp interactions and follows the power law E_ν^{-2} . The neutrinos from the relativistic jet cavities are emitted as precursors ($\sim 10 \div 100\text{s}$ prior) to the neutrinos emitted from the GRB fireball in case of electromagnetically observed burst [138]. In case of electromagnetically undetectable burst it is not possible to detect neutrinos from individual sources since a diffuse neutrino signal is spread all around.

- The *prompt emission* from GRBs can be correlated to the observed flux of Ultra High Energy Cosmic Rays (UHECRs), since protons are accelerated in the highly relativistic shocks by Fermi mechanism [44, 45, 47]. Such process implies the neutrino production through photon-hadronic interactions.
- *Afterglow neutrinos* are produced during the interaction between internal shocks from the original fireball and the interstellar medium [137]. Neutrinos are produced in the external reverse shock due to the interaction of shock accelerated protons with synchrotron soft X -ray photons.

In the GRB jet, a considerable number of neutrons ($n_n \simeq n_p$) is expected, arising from a neutronized core similar to that in supernovae in the case of long GRBs, and from neutron star material in the case of short GRBs. In a long GRB, the core collapse neutronization leads to huge amount of thermal neutrinos (~ 10 MeV). Due to their low energy, their cross section is too small for to be detected at cosmological distances. However, in both long and short GRB outflows, neutrons are present and initially coupled to protons by nuclear elastic scattering. If the initial acceleration of the fireball is very high, neutrons can eventually decouple from the fireball when the comoving expansion time falls below the nuclear scattering time. Protons, on the other hand, continue accelerating and expanding with the fireball as they are coupled to electrons by Coulomb scattering. The flux and the spectrum of EeV neutrinos depends on the density of the surrounding gas, while TeV-PeV neutrinos depend on the fireball Lorentz factor. Hence, the detection of very high energy neutrinos would provide crucial constraints on the fireball parameters and on GRB environment. Lower energy ($< \text{TeV}$) neutrinos originating from sub-stellar shocks, on the other hand, may provide useful information on the GRB progenitor.

Many experiment are searching neutrinos by GRBs. The AMANDA search, relied on spatial and temporal correlations with photon observations of other instruments, such as BATSE, CGRO [140] and other satellites of the Third InterPlanetary Network (IPN) [128], leads to an increase in sensitivity to a level where a single detected neutrino from a GRB can be significant at the 5σ level [139]. The neutrino flux limit from AMANDA data as presented in [141] is consistent with the flux predicted in [47]:

$$\Phi^{DL} = 6 \cdot 10^{-9} \text{ GeV cm}^{-2} \text{ s}^{-1} \text{ sr}^{-1}. \quad (5)$$

The expected number of detected events from a given GRB is quite low, however burst parameters can vary significantly from burst to burst leading to a large variation in the expected number of detected events. Thus the individual analysis of data from exceptionally bright GRBs is highly interesting. The AMANDA detector searched for neutrino emission from more than 400 GRBs, during the 1997 \div 2003 data taking. The coincidence time was assumed to be the whole emission duration over an excess of the background, while simulation-based data quality cuts were applied to separate the predicted signal from the observed background events. Zero neutrino events were observed in coincidence with the bursts, resulting in a stringent upper limit on the muon neutrino flux from GRBs [142–146]. IceCube [147] performed searches for neutrinos from GRBs with two analyses. In the first case, as for AMANDA, the selection of events was made using IPN-3-detected bursts as triggers on the prompt γ -ray emission of GRBs. However, since this kind of search misses all GRBs which are not in the field of view of satellites or do not emit gamma rays, a second analysis, seeking for unexpected temporal clustering of events was performed. In this analysis, a time window with a width fitting of the expected neutrino emission duration (typically between 1s and 100s) is imposed over the detected events comparing the observed number of events with those expected for the background. In 2008 IceCube, in a 22-string configuration, performed an analysis of individual GRB 080319B, the brightest GRB ever recorded, finding no significant neutrino excess above the background leading to the 90% upper limit neutrino flux [147]. However even for a 10 times larger telescope the number of expected event is only of the order of 1. Therefore, since the mean number of expected neutrinos from individual GRBs is usually small, IceCube performed a stacked GRB search, consisting in stacking several GRB events coming from different directions. In this way, the chance for discovery is noticeably enhanced, however it is no more possible to associate the neutrino flux to a specific GRB. An analysis with such an approach was performed with IceCube data: the neutrino spectra were calculated for 117 bursts (mainly detected by SWIFT and FERMI [148]) that occurred during data taking. Even in this case the data analysis showed no excess above the background.

The RICE experiment had investigated five bursts with respect to a possible flux connected to the afterglow emission [149], with limits of a few orders of magnitude above the prediction, derived for each burst individually [137]. Stacking more bursts, it can be possible to improve such limits.

The SuperKamiokande Collaboration performed a search for neutrinos based on a time and direction correlation analysis with BATSE GRB solar neutrinos, atmospheric neutrinos, and upward-going muon data samples aimed at the search for an excess in the number of events correlated with GRBs above the expected background [150]. Even in this case no statistically significant coincidences were observed and only an upper limit on the fluence of neutrino-induced muons has been set.

An analysis aimed to the detection of neutrino-induced showers in coincidence with GRBs using the ANTARES detector, complementary to the track searches typically performed in neutrino telescope experiments, was performed

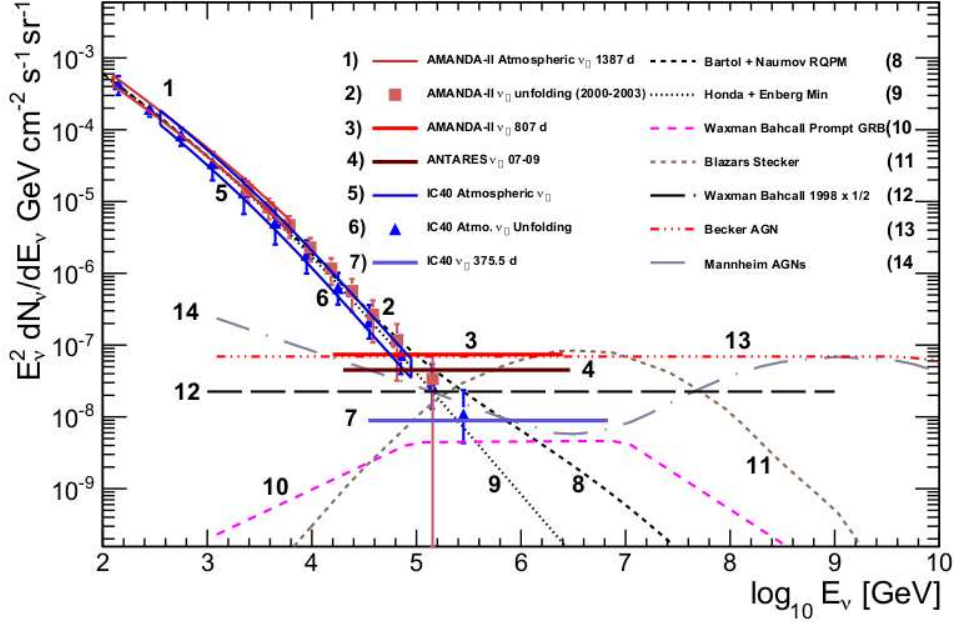


Figure 3: Upper limits on an astrophysical ν_μ flux with an E^{-2} spectrum are shown along with theoretical model predictions of diffuse astrophysical muon neutrinos from different sources. The astrophysical E^{-2} ν_μ upper limits are from AMANDA-II, ANTARES, and the current work utilizing the IceCube 40-string configuration (IC40 ν_μ 375.5 d). The atmospheric ν_μ measurements are from AMANDA-II, the IceCube 40-string (IC40) unfolding measurement and the current work (IC40 Atmospheric ν_μ) ([153] and references therein).

[151]. This method has a lower sensitivity per burst with respect to the track search, however it can detect neutrinos of any flavor, which are invisible for track based analysis, and it is capable of looking also for coincidences with GRBs occurring in the northern hemisphere, as it does not depend on the direction of the observation. Ten GRBs triggered during the year 2008 have been analyzed and no signal event were observed within the time-window. An upper limit on the normalization of this flux has been established [151].

Recently, the GRB fireball neutrino flux calculation has been revised taking into account the full spectral (energy) dependencies of the proton and photon spectra, as well as the cooling of the secondaries, flavor mixing, and additional multi-pion, kaon, and neutron production channels for the neutrinos [152]. A significant deviation has been found in the normalization of the neutrino flux prediction of about one order of magnitude, with a very different spectral shape peaking at slightly higher energies. With this approach, neutrino flux prediction is significantly below the current IceCube limit, which means that the conventional GRB fireball phenomenology is not yet challenged.

B. Gamma Ray Bursts and Gravitational waves

The main GRB models invoke a rapidly accreting black hole, formed during a violent event such as the core collapse of a massive compact star or the merger of two inspiraling binary neutron stars associated to a strong emission of gravitational wave signals. Whereas the γ -rays are thought to be produced at distances 10^{13} cm from the central engine, these gravitational waves will be produced in or near the central engine, and thus could provide our most direct probe of it. For example, collapse or merger models lead to different gravitational wave (GW)-burst energies, spectra, and polarizations [38–40, 154, 155]. Alternatively, GW production, owing to toroidal instabilities in an accretion disk, will be relatively long-lived and quasi-periodic, with an energy output of several orders of magnitude higher than in the accretion mechanism was proposed in [38]. In each case, the relative arrival time of GWB and GRB signals will depend on whether the GRB is generated by internal shocks in the exploding fireball or external shocks when the fireball is decelerated by the interstellar medium. In addition, GRBs occur at the rate of almost 1 observable event per day and are well localized in time and, very often, on the sky, to follow up GW searches. They are considered among the most promising GWs sources for ground-based interferometers, of the current and future generation, such as LIGO (Laser Interferometer Gravitational-Wave Observatory) [156, 157] and VIRGO [158] and their advanced versions. Although, with the current detector sensitivities, the cosmological distances of most GRBs

would lead to individually undetectable GW signals, it is possible to accumulate weak signals from several GRBs to detect a GW signature associated to the GRB population. Several Authors have described how the signals from two independent GW-detectors can be analyzed to identify the GW signals associated to GRBs and either bound or measure the population average of the GW-flux on Earth from this potential source. The key idea is to compare the mean correlated output of the detectors during GRB events ("on" times) to the mean correlated output when no GRB is detected ("off" times). Since gravitational waves from GRBs would produce small correlations in the output of the two detectors, a statistically significant difference in the mean correlated output between on and off times would constitute an indirect detection of GW-burst from GRBs. Alternately, the absence of a statistically significant difference would allow one to set an upper limit on the strength of any gravitational waves associated with GRBs. Long-duration GRBs is thought to follow the star formation rate of the Universe, and recent redshift measurements tend to support this model, with the measured GRB redshift distribution peaking at $z \simeq 1$. Long-duration GRBs have also been associated exclusively with late-type star-forming host galaxies. On the other hand, the recent observations of X-ray and optical afterglows from a few short-duration bursts seem to suggest that these GRBs are located at lower redshifts relative to long-duration GRBs, and that short bursts are found in a mixture of galaxy types, including elliptical galaxies, which have older stellar populations. Although a large fraction of GRBs are too distant for any associated GW signals to be detected by LIGO, it is plausible that a small fraction occur at closer distances. For example, a redshift of $z = 0.0085$, *i.e.* a distance of 35 Mpc, has been associated with long-duration burst/supernova GRB 980425/SN [159].

It is reasonable to expect that a few GRBs with no measured redshifts could be located relatively nearby as well. Long duration GRBs can last over several tens of seconds, with the time of peak flux appearing later than the time of first detection of GRB emission. This fact becomes important in the case of the internal shock models for GRB emissions since the delay of 0.5 sec between the GRB and the GW signal that is expected to be much smaller than the duration of the γ -ray light curve itself. In case of a long GRB, due to the missing of an accurate prediction of signal, analysis technique implemented by GW-detectors do not rely on a detailed prediction on the waveform, but only impose general bounds on signal duration and frequency.

For short GRBs, the redshift observations have led to fairly optimistic estimates [160, 161] for an associated GW observation in an extended LIGO science run. In fact observations support the hypothesis that a large fraction of short GRBs can be produced by NS-NS or NS-BH coalescence. Since, GWs measurements of well-localized inspiraling binaries can measure absolute source distances with high accuracy, simultaneous observations of GWs (emitted by binary systems) and short GRBs would allow us to directly and independently determine both the luminosity distance and the redshift of binary systems (see [162] and references therein). The combined electromagnetic and gravitational view of these objects is likely to teach us substantially more than what we learn from either data channel alone. In [162], the chirp masses associated to a sample of short GRBs (under the hypothesis that they are emitted by binary systems whose redshifts can be estimated considering them comparable to the GRB redshift) is obtained. In such a way, considering the coalescing time of the order of T_{90} -characteristic time¹ and the energy lost (during the final phase of the coalescing process) equal to the emission of short GRBs, it has been found that the chirp masses, obtained by simulations, are comparable to the theoretical chirp masses associated to the coalescing binary systems. Next generation of interferometers (as LISA [163], or Advanced-VIRGO and LIGO) could play a decisive role in order to detect GWs from these systems. At advanced level, one expects to detect at least tens NS-NS coalescing events per year, up to distances of order 2 Gpc, measuring the chirp masses with a precision better than 0.1%.

VI. GAMMA RAY BURST RADIO EMISSION

In the fireball model, GRB afterglows are the result of a shock pushed into the ambient medium by an extremely relativistic outflow from the GRB [164]. It has been suggested that a possible signature of exploding fireball is a burst of coherent radio emission [165].

The coherent radio emission is practically simultaneous with the GRB except for the reduced propagation speed of the radio waves by interstellar dispersion. A maximum delay of a few seconds has been predicted in [166] for galactic GRBs. Another coherent radio emission produce a cloud of Compton electrons propagating into the ambient magnetic field and radiating coherent synchrotron emission for roughly one gyroperiod. Since the radiation field of this emission process cannot exceed the ambient magnetic field, it is undetectable at cosmic distances [167].

In general, GRB afterglow observations are in good agreement with the external shock scenario. Light curves at

¹ T_{90} is defined as the time interval over which 90% of the total background-subtracted counts are observed, with the interval starting when 5% of the total counts have been observed.

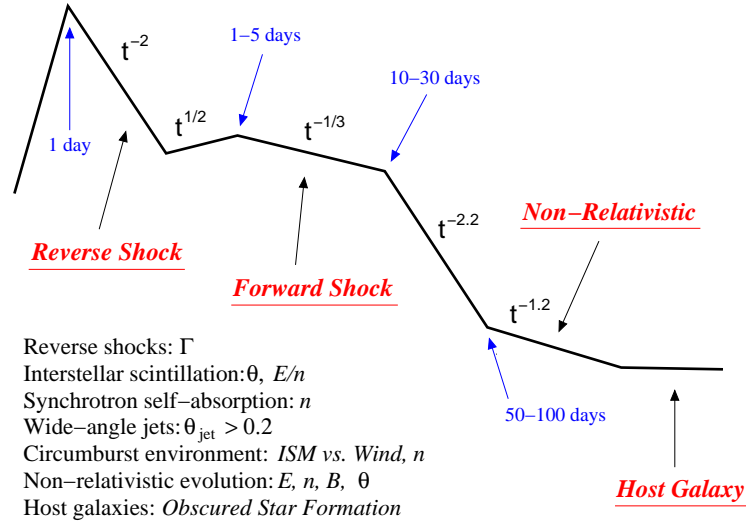


Figure 4: A schematic radio afterglow light curve. Timescales and scalings for the temporal evolution are indicated. The list summarizes aspects of the flux evolution which are unique to the radio bands (Lorentz factor, Γ ; source size, θ ; energy, E ; density, n ; jet opening angle, θ_{jet} ; density profile; magnetic field strength, B ; and obscured star formation rate)[168].

various wavelengths have been obtained for some bursts, and from these light curves, broadband spectra have been constructed. For the broadband spectrum, synchrotron radiation is assumed as the radiation mechanism. Dynamics of relativistic shock determines the spectrum evolution with time. The broadband synchrotron spectrum is determined by the peak flux and three break frequencies, namely the synchrotron self-absorption frequency ν_a , the frequency ν_m , that corresponds to the minimal energy in the electron energy distribution, and the cooling frequency ν_c that corresponds to electrons that cool on the dynamical timescale.

The break frequencies and the peak flux can be described in terms of energy of the blast-wave E , the density of the surrounding medium n , the fractional energy densities behind the relativistic shock in electrons and in the magnetic field, ϵ_e and ϵ_B respectively, the slope p of the electron energy distribution, and the jet opening angle θ_{jet} . Modeling radio emission provides the possibility to investigate the immediate surroundings of the burst and the initial Lorentz factor of blast-wave. The fact that the timescale for detecting emission from the reverse shock is small at optical and much longer at radio wavelengths makes radio observations on the first day after the burst important, although the emission from the forward shock is maybe not detectable at those early times.

The uniqueness of radio afterglow observations is best illustrated by the phenomenon of radio scintillation. Scintillation due to the local interstellar medium modulates the radio flux of GRB afterglows and permits indirect measurement of the angular size of the fireball. Focusing and defocusing of the wave front by large-scale inhomogeneities in the ionized interstellar medium results in refractive scintillation [168]. This scintillation is broadband and has been seen in many sources, whereas only the most compact sources, *e.g.* GRB afterglows, show diffractive scintillation. Diffractive scintillation is caused by interference between rays diffracted by small-scale irregularities in the ionized interstellar medium. The resulting interference is narrow-band and highly variable. Diffractive scintillation occurs only when the source size is smaller than a characteristic size, the so-called diffractive angle. It turns out that at an average redshift of $z \sim 1$, the size of the blast-wave is smaller than the diffractive angle in the first few days, but during its evolution the blast-wave becomes larger than this angle. Thus, as the blast-wave expands, the diffractive scintillation is quenched. By studying the scintillation behavior, one can get an independent measurement of the angular size of the blast-wave. The radio light curves are phenomenological different from optical and X -ray light curves in the sense that the flux at radio wavelengths first increases at a timescale of weeks to months before it starts to decline. Since X -ray afterglows are very weak, and optical afterglow observations are contaminated by the presence of a host galaxy or a possible supernova, radio afterglows provide essential informations in late-time, following GRBs in their evolution into the non-relativistic phase. These late-time observations can give a determination of the blast-wave energy independent of the initial jet collimation. Moreover they allow to observe phenomena which would otherwise escape attention, such as the occurrence of a radio flare.

The evolution a GRB and its radio afterglow is modelled schematically in Fig. 4. The observations cover four orders of magnitude in time ($0.1 \div 1000$ days) and three orders of magnitude in frequency ($0.8 \div 660$ GHz), so that radio light curves exhibit a rich phenomenology.

On a timescale of days to weeks after the burst, the subsequent evolution of the radio afterglow (Fig. 4) can be

described by a slow rise to maximum, followed by a power-law decay. The radio peak is often accompanied by a sharp break in the optical (or X -ray) light curves [31, 108].

The most commonly accepted (but not universal) explanation for these achromatic breaks is that GRB outflows are collimated. The change in spectral slope, where the flux density is $F \propto t^\alpha \nu^\beta$, occurs when the Lorentz factor Γ of the shock drops below the inverse opening jet angle θ_{jet} .

Since the radio emission initially lies below the synchrotron peak frequency ν_m , the jet break signature is distinctly different than that at optical and X -ray wavelengths.

Then jet break is expected to give rise to a shallow decay $t^{-\frac{1}{3}}$. Another recognizable radio signature of a jet-like geometry is the *peak flux cascade*, in which successively smaller frequencies reach lower peak fluxes (*i.e.* $F\nu_m \propto \sqrt{\nu_m}$).

At sufficiently late times, when the rest mass energy swept up by the expanding shock becomes comparable to the initial kinetic energy of the ejecta (~ 100 days), the expanding shock may slow to non-relativistic speeds [51]. A change in the temporal slope is expected (Fig. 4) for a constant density medium, independent of geometry. Finally, the radio light curves at late times may flatten due to the presence of an underlying host galaxy. Most GRBs studied so far have optical/NIR hosts but only about 20% have been seen at centimeter and submillimeter wavelengths [169, 170]. This is an emerging area with a great potential of study but requires a sensitivity that only a few radio telescopes have, as Very Large Array (VLA) [171], Low Frequency Array (LOFAR) [172], and the forthcoming Square Kilometer Array (SKA) [173]. Such instruments allow to investigate the GRB radio afterglows at high redshifts including also the possibility of more energetic versions of these objects that may be associated with Population III stars. This can be important for broadband afterglow fits aimed at determining total energies and physical parameters of bursts, out to very high redshifts.

VII. CONCLUSIONS

GRBs are flashes of γ -rays associated with extremely energetic explosions that have been observed in distant galaxies. As discussed, they can be roughly separated into two classes [174], long GRBs (with $T_{90} \gtrsim 2$ s), associated to gravitational collapse of very massive stars, and short GRBs (with $T_{90} \lesssim 2$ s), associated to mergers of compact objects. GRBs have recently attracted a lot of attention as promising standardizable objects candidates to describe the Hubble diagram up to very high z , deep into the matter dominated era thus complementing SNeIa which are, on the contrary, excellent probes for the dark energy epoch. However, still much work is needed in order to be sure that GRBs can indeed hold this promise.

Searching for a relation similar to that used to standardize SNeIa has lead to different empirically motivated scaling relations for GRBs. Anyway there are still open issues related to the use of GRBs in cosmology:

- the low number of events: the samples of GRBs which can be used to constrain cosmological parameters through the discussed correlations are not so rich;
- the absence of GRBs at low redshift does not allow to calibrate the correlations and requires to adopt methods to fit the cosmological parameters in order to avoid the circularity problem.

Moreover, the lack of theoretical interpretation for the physics of these correlations represents a still open issue. The increase of the number of bursts which can be used to measure the cosmological parameters, and the possible calibration of the correlations would greatly improve the constraints that are presently obtained with few events and non-calibrated correlations. In order to use GRBs as a cosmological tools, through the above correlations, three fundamental parameters, *i.e.* E_{peak} , E_γ and θ_{jet} , should be accurately measured. On the other hand the $L_{iso} - E_{peak} - T_{0.45}$ does not require the knowledge of the afterglow emission because it completely relies on the prompt emission observables. The need to know the cosmological model to infer the luminosity distance for each GRB contrasts with the desire to constrain that same cosmological model (circularity problem). In the attempt to overcome this problem, one can take into account scaling relations and derive the Hubble diagram by different methods in order to estimate the luminosity distance [37].

Moreover, GRBs are powerful sources of high-energy neutrinos emitted in different phases according to the fireball model. A mechanism leading to higher (GeV) energy neutrinos in GRB is due to inelastic nuclear collisions. Proton-neutron inelastic collisions are expected, at much lower radii than radii where shocks occur, due to the decoupling of neutrons and protons in the fireball or jet phases. If the fireball has a substantial neutron/proton ratio, as expected in most GRB progenitors, the collisions become inelastic and their rate peaks where the nuclear scattering time becomes comparable to the expansion time. Inelastic neutron/proton collisions then lead to charged pions, GeV muon and electron neutrinos. The typical GRBs neutrino energies range from multi-GeV to EeV, and can yield interesting physical information about fundamental interactions, about (ultra-high energy) cosmic rays, and about the nature

of GRBs and their environment. The GRBs neutrino signals may be detected in the coming years by current and forthcoming experiments such as Ice-Cube, RICE, and KM3NeT [175]. While the π interactions leading to > 100 TeV energy neutrinos provide a direct probe of the internal shock acceleration process, as well as of the MeV photon density associated with them, the > 10 PeV neutrinos would probe the reverse external shocks, as well as the photon energies and energy density there. In the very recent years several neutrino telescopes are performing a systematic search for neutrinos emission from GRBs with different analysis methods. Up to now, no signal in excess over the background rate has been observed.

The leading models for the ultimate energy source of GRBs are stellar collapse or compact stellar mergers, and these are expected to be sources of GWs. If some fraction of GRBs are produced by double neutron star or neutron star-black hole mergers, the gravitational wave chirp signal of the in-spiral phase should be detectable by the advanced LIGO-VIRGO, associated with the GRB electromagnetic signal. Although the waveforms of the gravitational waves produced in the break-up, merger and/or bar instability phase of collapsars are not known, a cross-correlation technique can be used making use of two co-aligned detectors.

The understanding of GRB physics is today rapidly advancing since the discovery of long-lived "afterglow" emission is giving a great insight into the problem. Radio afterglow studies have become an integral part of this field, providing complementary and sometimes unique diagnostics on GRB explosions, their progenitors, and their environments. The reason for this is that the radio part of the spectrum is phenomenologically rich, but also difficult to investigate because only 20% of GRBs observed so far have been seen at radio-wavelength. A GRB radio-survey requires a very high sensitivity that only few radio telescopes can reach. The forthcoming Square Kilometers Array (SKA) could be of extreme interest in this effort.

Acknowledgements

The Authors acknowledge L. Amati, G. Barbarino, V.F. Cardone, M.G. Dainotti, T. Di Girolamo and M. Perillo for useful discussions and comments on topics related with this paper.

-
- [1] P. de Bernardis, P.A.R. Ade, J.J. Bock, J.R. Bond, J. Borrill, et al., *Nature*, **404**, 955 (2000).
 - [2] M.L. Brown, P. Ade, J. Bock, M. Bowden, G. Cahill, et al., *ApJ* **705**, 978 (2009).
 - [3] E. Komatsu, K.M. Smith, J. Dunkley, C.L. Bennett, B. Gold, B. et al. , *ApJS* **192**, 18 (2011).
 - [4] S. Dodelson, V.K. Narayanan, M. Tegmark, R. Scranton, T. Budavari, et al., *ApJ* **572**, 140 (2002).
 - [5] W.J. Percival, W. Sutherland, J.A Peacock, C.M. Baugh, J. Hawthorn, J. et al. , *MNRAS* **337**, 1068 (2002).
 - [6] A.S. Szalay, et al., *ApJ* **591**, 1 (2003).
 - [7] E. Hawkins, S. Maddox, S. Cole, O. Lahav, D.S. Madgwick, et al., *MNRAS* **346**, 78 (2003).
 - [8] D.J. Eisenstein, I. Zehavi, D.W. Hogg, R. Scoccimarro, M.R. Blanton, et al., *ApJ* **633**, 560 (2005).
 - [9] W.J. Percival, B.A. Reid, D.J. Eisenstein, N.A. Bahcall, T. Budavari, et al., *MNRAS* **401**, 2148 (2010).
 - [10] M. Kowalski, D. Rubin, G. Aldering, R.J. Agostinho, A. Amadon, A. et al., , *ApJ* **686**, 749 (2008).
 - [11] M. Hicken, W.M. Wood-Vasey, S. Blondin, P. Challis, et al., *ApJ* **700**, 1097 (2009).
 - [12] R. Kessler, A.C Becker, et al., *ApJS* **185**, 32 (2009).
 - [13] S.M. Carroll, W.H. Press, E.L. Turner, *ARAA* **30**, 499 (1992).
 - [14] V. Sahni, A.A. Starobinsky, *Int. J. Mod. Phys. D* **9**, 373 (2000).
 - [15] P.J.E. Peebles, B. Ratra, *Rev. Mod. Phys.* **75**, 559 (2003).
 - [16] E.J. Copeland, M. Sami, S. Tsujikawa, **Int. J. Mod. Phys. D** **15**, 1753 (2006)
 - [17] S. Capozziello, M. Francaviglia, *Gen. Rel. Grav.* **40**,357, (2008);
 - [18] T.P. Sotiriou, V. Faraoni, *Rev. Mod. Phys.* **82**, 451 (2010);
 - [19] Nojiri, S., Odintsov, S.D. 2008, in *Problems of Modern Theoretical Physics*, A Volume in honour of Prof.I.L. Buchbinder in the occasion of his 60th birthday,p.266-285, TSPU Publishing, Tomsk preprint arXiv:0807.0685
 - [20] A. De Felice, S. Tsujikawa, *Living Reviews in Relativity* **3**, 3 (2010).
 - [21] S. Capozziello, M. De Laurentis, *Physics Reports* **509**, 167 (2011).
 - [22] S. Nojiri, S.D. Odintsov, *Int. J. Geom. Meth. Mod. Phys.* **4**, 115 (2007);
S. Capozziello, M. De Laurentis, M. Francaviglia, *Astrop. Phys.* **29** 125 (2008);
S. Capozziello, M. De Laurentis, V. Faraoni, *The Open Astr. Jour* , **2**1874, (2009);
S. Nojiri, S.D. Odintsov, *Phys.Rept.* **505**, 59 (2011).
 - [23] G. Aldering, W. Althouse, R. Amanullah et al., arXiv:astro-ph/0405232 (2004).
 - [24] R. Salvaterra, M. Della Valle, S. Campana, G. Chincarini et al. *Nature* **461**, 1258 (2009).
 - [25] L. Amati, C. Guidorzi, F. Frontera, M. Della Valle, F. Finelli, R. Landi, E. Montanari, *MNRAS* **391**, 577 (2008).
 - [26] F. Y. Wang, Z. G. Dai, *Astron. & Astroph.* **536**, A96 (2011).
 - [27] F. Y. Wang, S. Qi, Z. G. Dai, *MNRAS* **415**, 3423 (2011)

- [28] E.E. Fenimore, E. Ramirez - Ruiz, *ApJ* **539**, 712 (2000). G.
- [29] Ghirlanda, G. Ghisellini, D. Lazzati, D. *ApJ* **616**, 331 (2004).
- [30] E. Liang, B. Zhang, *ApJ* **633**, 611 (2005).
- [31] C. Firmani, G. Ghisellini, V. Avila - Reese, V., G. Ghirlanda, *MNRAS* **370**, 185 (2006).
- [32] N. Liang, W.K. Xiao, Y. Liu, S.N. Zhang, S.N. *ApJ* **385**, 654 (2008).
- [33] N. Liang, P. Wu, S.N. Zhang, *Phys. Rev. D* **81**, 083518 (2010).
- [34] S. Qi, T. Lu, *ApJ* **717**, 1274 (2011).
- [35] S. Capozziello, L. Izzo *A&A* **490**, 31 (2008).
- [36] L. Izzo, S. Capozziello, G. Covone, M. Capaccioli, *A&A* **508**, 63 (2009).
- [37] V.F. Cardone, M. Perillo, S. Capozziello, *MNRAS* **417**, 1672 (2011).
- [38] P. Meszaros, *Rept. Prog. Phys.*, **69**, 2259 (2006).
- [39] P. Meszaros, S. Kobayashi, S. Razzaque, B. Zhang, arXiv: astro-ph/0305066 (2003).
- [40] P. Meszaros, S. Razzaque, arXiv:astro-ph/0605166 (2006).
- [41] Kouveliotou, C. Meegan, C.A. Fishman et al., *ApJ* **413**, L101 (1993).
- [42] N. Gehrels, et al., *Nature* **444**, 1044. (2006).
- [43] E. Waxman, *Phys. Rev. Lett.* **75**, 386 (1995).
- [44] M. Vietri, *ApJ* **453**, 883 (1995).
- [45] E. Waxman and J. Bahcall, *Phys. Rev. D* **59**, 023002 (1999).
- [46] J. Bahcall and E. Waxman, *Phys. Rev. D* **64**, 023002 (2001).
- [47] E. Waxman and J. Bahcall, *Phys. Rev. Lett.* **78**, 2292 (1997).
- [48] T. Piran, *Phys. Rep.* **314**, 575 (1999).
- [49] M. H.P.M. van Putten *ApJ* **579**, L63 (2002).
- [50] M. B. Davies, A. King et al. astro-ph/0204358 (2002).
- [51] T. Piran *Rev. Mod. Phys.* **76**, 1143 (2004).
- [52] R. Klebesadel, I. Strong, & R. Olson, *ApJ* **182**, L85 (1973).
- [53] J.P. Dezalay et al. *Astrophys. J. Lett.* **471**, L27 (1996).
- [54] C. Kouveliotou et al. *ApJ* **413**, L101 (1993).
- [55] D.A. Kann et al., *ApJ* **734**, 96 (2011).
- [56] E. Nakar, *Phys. Rep.*, **442**, 166 (2007).
- [57] R. C. Duncan, C. Thompson, *ApJ* **392**, L9 (1992).
- [58] E. Nakar, A. Gal-Yam, D.B. Fox, *ApJ* **650**, 281 (2006).
- [59] R. Chapman, R.S. Priddey, and N.R. Tanvir, *AIP Conf. Proc.*, **983**, 304 (2008).
- [60] T.J. Galama, et al., *Nature* **395**, 670 (1998).
- [61] J. Hjorth, et al., *Nature* **423**, 847 (2003).
- [62] D. Malesani, et al., *ApJ* **609**, L5 (2004).
- [63] S. Campana, et al., *Nature* **442**, 1008 (2006).
- [64] C.L. Fryer, S.E. Woosley, D.H. Hartmann, *ApJ* **526**, 152 (1999).
- [65] J.K. Cannizzo, N. Gehrels, *ApJ* **700**, 1047 (2009).
- [66] M. De Pasquale et al., *ApJ* **592**, 1018 (2003).
- [67] A. J. van der Horst, R. A. M. J. Wijers, E. Rol, *Nuovo Cim. C* **28**, 467 (2005).
- [68] J. Heise, J. in't Zand, R. Kippen, P. Wood in *Gamma-ray Bursts in the afterglow era*, ed. E. Costa, F. Frontera & J. Hjorth (Brelm: Springer) **16** (2001).
- [69] B. Gendre et al. *AAP* **462**, 565 (2007).
- [70] B. Gendre, arXiv: 0807.3918 (2008).
- [71] M.J. Rees, P. Meszaros *MNRAS* **258**, P41 (1992).
- [72] T. Piran, *Ap. J. Lett.*, **389**, L45 (1992).
- [73] V. D'Alessio, L. Piro, E.M. Rossi *AAP* **460**, 653 (2006).
- [74] V.V. Usov, *Nature* **357**, 472 (1992).
- [75] B.E. Schaefer, *ApJ*, **583**, L67 (2003).
- [76] B.E. Schaefer, *ApJ*, **660**, 16 (2007)
- [77] B. Zhang, P. Meszaros *Internat. J. Mod. Phys. A* **19**, 2385 (2004).
- [78] S. Weinberg "Gravitation and Cosmology", John Wiley & Sons, Inc., New York, (1972).
- [79] G. Ghirlanda, G. Ghisellini and C. Firmani, *New Journal of Physics* **8**, 123 (2006).
- [80] S. Basilakos, L. Perivolaropoulos, *MNRAS* **391**, 411 (2008).
- [81] R. Preece et al., *ApJS* **126** 19 (2000).
- [82] D.A. Frail, S.R. Kulkarni and R. Sari, *ApJ* **562**, L55 (2001).
- [83] J.S. Bloom, D.A. Frail and S.R. Kulkarni, *ApJ* **594** 674 (2003).
- [84] E. Waxman, S.R. Kulkarni and D.A. Frail, *ApJ* **497**, 288 (1998).
- [85] A. Fruchter et al., *ApJ* **519**, L13 (1999).
- [86] J.A. Rhoads et al., *ApJ* **487** L1 (1997).
- [87] R. Sari, T. Piran and J.P. Hapler *ApJ* **519** L17 (1999)
- [88] A. Dar, *Astrophys. S.* **138** 505 (1999).
- [89] <http://www.batse.msfc.nasa.gov/batse/>
- [90] J.P. Norris *ApJ* **579**, 386 (2002).

- [91] L. Chen et al., *ApJ* 619 983 (2005).
- [92] L.A. Ford et al., *ApJ* 439 307 (1995).
- [93] D. Kocevsky and E. Liang, *ApJ* 594 ,385 (2003).
- [94] B.Wu and E.E. Fenimore, *ApJ* 535, L29 (2000).
- [95] F. Ryde *Astron. Astrophys.* 429 869 (2005).
- [96] R. F. Shen, L.M. Song and Z. Li, *MNRAS* 362, 59 (2005).
- [97] J. P. Norris,G.F. , Marani and J. T. Bonnel *ApJ* 534, 248 (2000).
- [98] D.L. Band, J.P. Norris and J.T. Bonnell, *ApJ* 613 484 (2004).
- [99] D. Bersier et al., *ApJ* 584, L43 (2003).
- [100] R. Sato et al., *ApJ* 599, L9 (2003).
- [101] D. Q. Lamb, C. Graziani and A. Smith *ApJ* 413, L11(1993).
- [102] C.D. Dermer and K. E. Mitman *it Nature* 513 L5 (1999).
- [103] E.E. Fenimore and E. Ramirez-Ruiz astro-ph/0004176 (2000)
- [104] D. Reichart et al., *ApJ* 552, 57 (2001).
- [105] C. Guidorzi et al., *MNRAS* 363, 315 (2005).
- [106] C. Guidorzi et al., *MNRAS* 364 163 (2005).
- [107] L.X. Li and B. Paczynski, *MNRAS* 366, 219 (2006).
- [108] B. Zhang and H. Yan *ApJ* 726, 90 (2011).
- [109] H. Gao, B.B. Zhang, B. Zhang, arXiv:1103.0074v3 [astro-ph.HE], (2011).
- [110] N. Lloyd and E. Ramirez-Ruiz, *ApJ.* 576, 101 (2002).
- [111] L. Amati et al., *Astron. Astrophys.* 390, 81 (2002).
- [112] <http://www.asdc.asi.it/bepposax/>
- [113] G. Ghirlanda, G. Ghisellini G and D. Lazzati, *ApJ* 616, 331(2004).
- [114] T. Sakamoto et al., *ApJ* 629, 311 (2005)
- [115] D.Q. Lamb, T.Q. Donaghy and C. Graziani, *New Astron. Rev.* 48 459 (2004).
- [116] L. Amati, *MNRAS* 372, 233 (2006).
- [117] D. Eichler and A. Lenvinson, *ApJ* 614, L13 (2004).
- [118] A. Levinson and D. Eichler *ApJ* 629, L13 (2005).
- [119] R. Yamazaki, K. Yoka and T. Nakamura *ApJ* 606, L33 (2004).
- [120] K. Toma, R. Yamazaki and T. Nakamura *ApJ* 635, 481 (2005).
- [121] M. J. Rees and P. Meszaros *ApJ* 628, 847 (2005).
- [122] D. Yonetoku et al., *ApJ* 609, 935 (2004).
- [123] G. Ghirlanda, G. Ghisellini and C. Firmani, *MNRAS* 361, L10 (2005).
- [124] L. Nava et al., *Astron. Astrophys.* 450, 471(2006).
- [125] E. Ramirez-Ruiz, *ApJ* 625, L91(2005).
- [126] D. Watson et al.,*ApJ* 636, 967 (2005).
- [127] <http://www.swift.psu.edu/>
- [128] <http://www.ssl.berkeley.edu/ipn3/>
- [129] B.E. Cobb et al., *ApJ* 645, L113 (2006).
- [130] Ghisellini G et al., *MNRAS* 372, 1699 (2006).
- [131] R.A. Chevalier and Z.Y. Li, *ApJ* 536 195 (2000).
- [132] S. Weinberg, *Gravitation and Cosmology*, Wiley, New York (1972).
- [133] M. Visser, *Class. Quant. Grav* 21, 2603 (2004).
- [134] Y. Kodama, D. Yonetoku, T. Murakami, S. Tanabe, R. Tsutsui, T. Nakamura, *MNRAS* 391, L1 (2008).
- [135] H. Wei, S.N. Zhang, *Eur. Phys. Journ. C* 63, 139 (2009).
- [136] S. Razzaque, P. Mészáros, and E. Waxman, *Phys. Rev. D*, 68, 083001, (2003).
- [137] E. Waxman and J. N. Bahcall, *ApJ.* 541, 707 (2000).
- [138] J. K. Becker, *Phys. Rept.* 458 173 (2008).
- [139] <http://amanda.uci.edu/>
- [140] <http://heasarc.gsfc.nasa.gov/docs/cgro/egret/>
- [141] A. Achterberg, (IceCube Coll.), et al., *ApJ* 674, 357 (2008).
- [142] A. Achterberg, (IceCube Coll.), et al. IceCube contributions to *ICRC 2005*, astro-ph/0509330 (2005).
- [143] A. Achterberg, (IceCube Coll.), et al. In *J. of Phys.*, Conference Series, 2006. *astro-ph/0611597*;
<http://www.icecube.wisc.edu/tev/>.
- [144] A. Achterberg, (IceCube Coll. and P. L. Biermann), et al. *Astropart. Phys.* 26, 282 (2006).
- [145] A. Achterberg, (IceCube Coll.), et al. *ApJ* 664, 397 (2007).
- [146] A. Achterberg, (IceCube Coll.), et al. *Phys. Rev. D*, 75, 102001 (2007).
- [147] <http://icecube.wisc.edu/>
- [148] <http://fermi.gsfc.nasa.gov/>
- [149] D. Besson et al., *Astropart. Phys.*, 26, 367 (2007).
- [150] <http://www-sk.icrr.u-tokyo.ac.jp/sk/index-e.html>
- [151] <http://antares.in2p3.fr/>
- [152] S. Hummer, Ph. Baerwald, W. Winter, arXiv:1112.1076 [astro-ph.HE] (2012).
- [153] A. Achterberg, (IceCube Coll.), *Phys. Rev. D* 84, 082001 (2011).

- [154] M. Maggiore, *Gravitational Waves, Volume 1: Theory and Experiments*, Oxford Univ. Press (Oxford) (2007).
- [155] A. V. Tutukov, A. V. Fedorova, *Astron. Repts.* **51**, 291 (2007).
- [156] A. Abramovici, , et al., *Science*, **256**, 325 (1992).
- [157] A. Abbott, , et al., *Phys. Rev.*, **D 77**, 062004 (2008).
- [158] B. Caron et al., *Class. Quant. Grav.*, **14**, 1461 (1997).
- [159] T. J. Galama et al., *Nature* **395**, 670 (1998).
- [160] E. Nakar, A. Gal-Yam, and D. B. Fox, *ApJ* **650**, 281 (2006).
- [161] D. Guetta and T. Piran, *Astron. & Astrophys.* **453**, 823 (2006).
- [162] S. Capozziello, M. De Laurentis, I. De Martino, M. Formisano, *Astrophys.Space Sci.* **332**, 31 (2011).
- [163] <http://www.lisa-science.org>
- [164] A. O. Benz and G. Paesold, *Astron. Astrophys.* **329**, 61 (1998).
- [165] M.J. Rees, *Nature* **266**, 333 (1977).
- [166] Palmer D.M., *ApJ* **417**, L25 (1993).
- [167] J.I. Katz, *ApJ* **422** 248 (1994).
- [168] D. A. Frail, arXiv:astro-ph/0309557v1, (2003).
- [169] J.P. Dezalay et al., *Astrophys. J. Lett.* **471**, L27 (1996).
- [170] C. Kouveliotou et al. *ApJ* **413**, L101 (1993).
- [171] <http://www.vla.nrao.edu/>
- [172] <http://www.lofar.org/>
- [173] <http://www.skatelescope.org/>
- [174] T. Weekes, *Very High Energy Gamma-Ray Astronomy*(IoP), Bristol. (2003).
- [175] <http://www.km3net.org/>